Temperature-dependent surface relaxations of Ag(111)

Jianjun Xie*
Fritz-Haber-Institut der Max-Planck-Gesellschaft, Faradayweg 4-6, D-14195 Berlin-Dahlem, Germany

Stefano de Gironcoli
Scuola Internazionale Superiore di Studi Avanzati and Istituto Nazionale per la Fisica della Materia, via Beirut 2-4, I-34014 Trieste, Italy

Stefano Baroni
Scuola Internazionale Superiore di Studi Avanzati and Istituto Nazionale per la Fisica della Materia, via Beirut 2-4, I-34014 Trieste, Italy
and Centre Européen de Calcul Atomique et Moléculaire ENS, Aile LR5, 6, Allée d'Italie, 69007 Lyon, France

Matthias Scheffler
Fritz-Haber-Institut der Max-Planck-Gesellschaft, Faradayweg 4-6, D-14195 Berlin-Dahlem, Germany
(Received 28 May 1998)

The temperature-dependent surface relaxation of Ag(111) is calculated by density-functional theory. At a given temperature, the equilibrium geometry is determined by minimizing the Helmholtz free energy within the quasiharmonic approximation. To this end, phonon dispersions all over the Brillouin zone are determined from density-functional perturbation theory. We find that the top-layer relaxation of Ag(111) changes from an inward contraction (-0.8%) to an outward expansion ($+6.3\%$) as the temperature increases from $T=0$ K to 1150 K, in agreement with experimental findings. Also, the calculated surface phonon dispersion curves at room temperature are in good agreement with helium-scattering measurements. The mechanism driving this surface expansion is analyzed, and the physical picture developed by Narasimhan and Scheffler is essentially confirmed. [S0163-1829(99)00502-0]

I. INTRODUCTION

The equilibrium geometry of a system depends on the temperature due to the anharmonicity of the interatomic potential. The presence of a surface breaks the periodic structure normal to the surface, and anharmonic effects are expected to be larger at the surface than in the bulk.[1] Hence, the surface interlayer separation may change more strongly with temperature than the bulk lattice parameter. Indeed, enhanced anharmonic effects have been observed by recent experiments on several surfaces: Ni(001),[2] Pb(110),[3] Cu(110),[4] Ag(111),[5] Cu(111),[6] as well as Be(0001).[7] Among them, the large thermal expansion observed in the close-packed Ag(111) surface has attracted much attention,[8–10] but at present the interpretation of these results is still controversial.

Using an the embedded-atom method (EAM) in which the parameters of the interatomic potential are determined by fitting bulk properties, Lewis[8] simulated the thermal behavior of Ag(111) for a large range of temperatures using molecular dynamics. The results for the top layer relaxation differ significantly from those reported by an experimental study:[5] the top interlayer spacing, d_{12}, remains smaller than the bulk value even at temperatures as high as 1110 K; while the analysis of experimental results[5] obtained by the medium energy ion scattering (MEIS), concluded that d_{12} changes from -2.5% contraction to 10.0% expansion as temperature increases from room temperature to 1150 K. Narasimhan and Scheffler[9] investigated the temperature dependence of d_{12} by minimizing the Helmholtz free energy of the system with respect to d_{12} in a simplified quasiharmonic approximation (QHA), where the vibrational free energy was calculated including only three representative modes corresponding to the rigid vibration of the top layer on a rigid substrate. The static total energy and the vibrational frequencies, were calculated using density-functional theory (DFT) within the local-density approximation (LDA). Although the results obtained within this ''three-mode approximation'' overestimated the effect (e.g., at $T=1040$ K, the calculated surface relaxation is 15% whereas the experimental value was 7.5%), these calculations provided a *physical explanation* of the mechanism underlying the thermal expansion observed at this surface. Subsequently, using again EAM potential, Kara *et al.*[10] obtained a rather small thermal expansion. They argued that the large thermal expansion of Ref. 9 was the result of an improper representation of the vibrational density of states. On the other hand, very recent MEIS measurements on Cu(111) (Ref. 6) and LEED measurements on Be(0001) (Ref. 7) seem to support the theoretical picture developed in Ref. 9.

Recent calculations of the thermal properties of Ag bulk[11] demonstrate that the QHA provides a very accurate description of the thermal expansion and heat capacity of Ag up to the melting point. In order to resolve the controversy on the thermal behavior of Ag(111), we have recalculated the surface thermal expansion of this surface within DFT-LDA and QHA without any further approximations. In particular, the vibrational contributions to the free energy from the whole

Brillouin zone (BZ) are included thanks to the efficient calculation of phonon dispersions by density-functional perturbation theory.[12] Our results positively indicate that DFT and the QHA—at variance with previous attempts based on EAM (Refs. 8 and 10)—provide a *quantitatively* correct description of the anomalous thermal properties of this surface. Our results also show the importance of a proper sampling of vibrational modes over the BZ for a quantitatively reliable result. The *qualitative* explanation of the earlier work of Narasimhan and Scheffler[9] is fully confirmed. The disagreement with reported EAM results[8,10] is argued to due to the approximate nature of EAM and to an incorrect **k**-point summation in Ref. 10.

II. COMPUTATIONAL DETAILS

To model the surface, we adopt a repeated-slab geometry consisting of seven atomic layers separated by a vacuum region corresponding to five atomic layers. As in a previous treatment,[13] the Helmholtz free energy of the slab is given by

$$\begin{aligned} F(\{d\},T) &= E(\{d\}) + F_{\mathrm{vib}}(\{d\},T) \\ &= E(\{d\}) + k_{\mathrm{B}}T \sum_{\mathbf{q}_\parallel} \sum_{p=1}^{3N} \\ &\quad \times \ln\left\{ 2\sinh\left(\frac{\hbar\omega_p(\mathbf{q}_\parallel,\{d\})}{2k_{\mathrm{B}}T} \right) \right\}, \end{aligned} \tag{2.1}$$

where E is the static total energy, as obtained by DFT calculations, k_{B} and $\hbar$ are the Boltzmann and the Planck constants, and $\{d\}$ represents the set of interlayer distances normal to the surface and the interparticle distances parallel to the surface. The vibrational free energy is denoted as F_{vib}, and $\omega_p(\mathbf{q}_\parallel,\{d\})$ is the frequency of the pth mode for a given wave vector $\mathbf{q}_\parallel$, evaluated at the geometry defined by $\{d\}$; and N is the number of atoms in the slab. The static total energy E in Eq. (2.1) includes all the anharmonic terms of the interatomic potential. The anharmonic nature also appears in the vibrational free energy F_{vib} since in the quasiharmonic approximation the vibrational frequencies $\omega_p(\mathbf{q}_\parallel,\{d\})$ are allowed to change with $\{d\}$.

At a given temperature T and zero pressure, the equilibrium geometry is determined by the minimum of the Helmholtz free energy, i.e., $\partial F/\partial d = \partial E/\partial d + \partial F_{\mathrm{vib}}/\partial d = 0$. It is not practical to minimize the Helmholtz free energy with respect to all the lattice parameters $\{d\}$ within the present *ab initio* approach. Remember the facts that the translational symmetry of the crystal still remains along the direction parallel to the surface and the relaxation of the deep layer is usually small, we therefore assume here that the temperature dependence of the in-plane lattice constant as well as other out-of-plane interlayer distances (denoted as $\{d'\}$) except the top layer spacing d_{12} is the same with the bulk.[11] The temperature dependent equilibrium d_{12} is then determined by

$$\begin{aligned} \frac{\partial E(\{d_{12},d'\})}{\partial d_{12}} &= -\frac{\partial F_{\mathrm{vib}}(\{d_{12},d'\})}{\partial d_{12}} \\ &= -\sum_{\mathbf{q}} \sum_{p} \frac{\partial \hbar\omega_p(\mathbf{q},\{d_{12},d'\})}{\partial d_{12}} \\ &\quad \times n_p(\mathbf{q},\{d_{12},d'\}), \end{aligned} \tag{2.2}$$

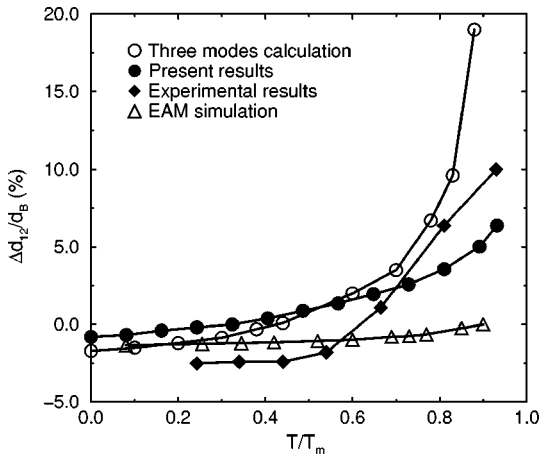

FIG. 1. Temperature dependence of surface layer relaxation of Ag(111). Our calculated results are denoted by the filled circles. Open circles are the results of Ref. 9; open triangles are EAM simulations (Ref. 10). The experimental results (Ref. 5) are shown by filled diamonds.

where n_p is the occupation number of the pth mode defined by

$$n_p(\mathbf{q},\{d_{12},d'\}) = \frac{1}{2} + \frac{1}{e^{\hbar\omega_p(\mathbf{q},\{d_{12},d'\})/k_{\mathrm{B}}T} - 1}. \tag{2.3}$$

It is noted that the variation of $\omega_p(\mathbf{q},\{d_{12},d'\})$ with d_{12} is different at different temperature due to the change of $\{d'\}$.

The static total energy E is calculated by density-functional theory within the local-density approximation.[14] Fully separable norm-conserving pseudopotentials[15] are used in our calculations together with a plane wave basis set with a kinetic energy cut-off of 55 Ry. BZ integrations are performed with the smearing technique of Ref. 16 using the Hermite-Gauss smearing function of order one, a smearing width $\sigma = 50$ mRy, and a 16-point grid in the irreducible wedge of the BZ. The phonon frequencies of the system are calculated by density-functional perturbation theory.[12] The dynamical matrices are calculated on a 4×4 grid of points in the surface BZ of the 7-layer slab and Fourier interpolated over a 48-point grid of $\mathbf{q}_\parallel$ vectors in the irreducible wedge of the surface BZ, in order to calculate the vibrational contribution to the free energy.

III. RESULTS

We first calculated the surface relaxation of Ag(111) by minimizing the static total energy and neglecting the vibrational contributions. The obtained results are $\Delta d_{12}/d_{\mathrm{B}} = -1.0\%$, $\Delta d_{23}/d_{\mathrm{B}} = -0.2\%$, where d_{B} is the interlayer spacing in the bulk. Starting from this static equilibrium geometry, the Helmholtz free energy of the slab is evaluated as a function of the interlayer interspacings $\{d\}$. The temperature dependence of the equilibrium d_{12} is then obtained from Eq. (2.2) in which all other interlayer spacings $\{d'\}$ including d_{B} are assumed to expand according to the temperature dependence of the bulk. Neglecting the temperature dependence of $\{d'\}$ will give even larger thermal expansion of d_{12}. Figure 1 shows the calculated results (filled circles) together with the experimental data[5] (filled diamonds) and

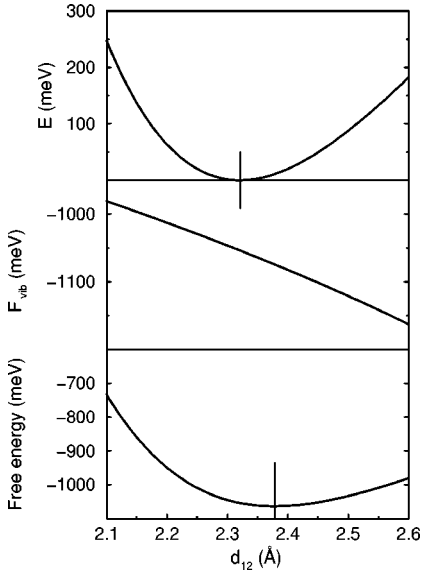

FIG. 2. Variation of the static total energy E, vibrational free energy F_{vib} and the Helmholtz free energy with the surface interlayer spacing d_{12} at $T=500$ K.

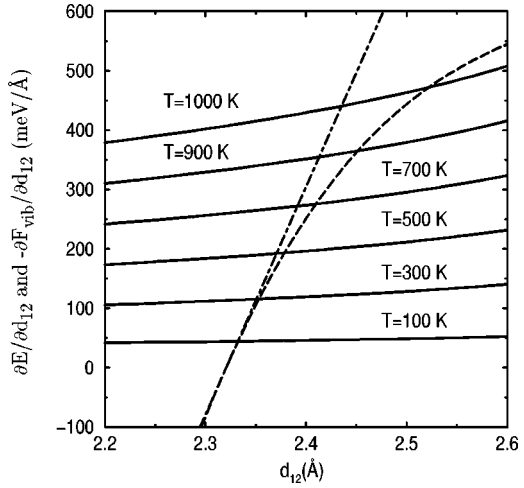

FIG. 3. Variation of $-\partial F_{\mathrm{vib}}/\partial d_{12}$ (solid lines) and $\partial E/\partial d_{12}$ (dashed line) with d_{12}. The harmonic results of $\partial E/\partial d_{12}$ are shown by the dot-dashed line. The equilibrium d_{12} is obtained by the intersection of the solid lines and the dashed line.

other calculations.[9,10] The temperature is scaled with respect to the experimental melting temperature [$T_{\mathrm{m}}=1234$ K (Ref. 17)]. It can be seen that in the low temperature range ($T/T_{\mathrm{m}}<0.6$), the present calculation gives a thermal expansion similar to that of Ref. 9. At higher temperatures, the calculations of Ref. 9 overestimate the thermal expansion of Ag(111). The present calculation, which includes all the vibrational modes of the slab in the whole BZ, displays a much smaller top layer expansion than obtained in the ''three-mode approximation,'' [9] thus bringing the theoretical predictions in much closer agreement with experimental results: $\Delta d_{12}/d_{\mathrm{B}}$ changes from -0.8% inward contraction (including zero-point vibrations) at $T=0$ K to $+6.3\%$ outward expansion at $T=1150$ K [the corresponding experimental figures vary from -2.5% to $+10.0\%$ (Ref. 5)]. The EAM simulation in Ref. 10, on the contrary, shows no enhancement of thermal expansion of the interlayer spacing in the whole temperature range, i.e., the d_{12} value always remains smaller than the interlayer spacing in the bulk.

What is the mechanism giving Ag(111) such an enhanced thermal expansion? Figure 2 shows the variation of the static energy, E, the Helmholtz free energy, F, and the vibrational free energy, F_{vib}, with the top-layer interspacing d_{12}, for $T=500$ K. The equilibrium geometry, d_{12}, is determined by two factors: one is the static total energy, E, which governs the binding strength of the surface with the substrate and the anharmonicity of the interlayer potential normal to the surface; the other is the decrease of the vibrational free energy, F_{vib}, which reflects the ''softening'' of the vibrational frequency with the increase of d_{12}. We note that F_{vib} does not always decrease with the increase of lattice parameters, for example, in the anomalous thermal expansion of bulk silicon.[18] As d_{12} increases from the static equilibrium value, d_{12}^{0}, the interlayer potential increases while the vibrational free energy decreases, determining a new equilibrium spacing d_{12}, larger than d_{12}^{0}. Figure 3 shows how the temperature dependent equilibrium d_{12} is obtained from Eq. (2.2). The dashed line is the variation of $\partial E/\partial d_{12}$ with d_{12}. The dot-dashed line is the derivative of E with respect to d_{12} when anharmonic terms in E are neglected by quadratically expanding it around the static equilibrium geometry. The solid lines are $-\partial F_{\mathrm{vib}}/\partial d_{12}$ at different temperatures. The equilibrium geometry of d_{12} is determined by the intersection of $\partial E/\partial d_{12}$ and $-\partial F_{\mathrm{vib}}/\partial d_{12}$. It can be clearly seen that by increasing the temperature, the intersection of $\partial E/\partial d_{12}$ and $-\partial F_{\mathrm{vib}}/\partial d_{12}$ gives an increasing value of equilibrium distance d_{12}. Furthermore, the anharmonicity of the static energy E, dashed line, is essential in determining the enhanced thermal expansion at high temperature, that would be much reduced if this anharmonicity were neglected (dot-dashed line).

The driving force for expansion comes from the temperature variation of the vibrational free energy. Equation (2.2) reveals that the value of $-\partial F_{\mathrm{vib}}/\partial d_{12}$ at a given temperature is determined by $\partial \hbar \omega_p/\partial d_{12}$ which represents the ''softening'' of ω_p with the increase of d_{12}. Such ''softening'' of the frequencies is characterized by the shift of the phonon density of states (DOS). Figure 4 shows the shift of layer localized phonon DOS with d_{12}. The solid line corresponds to $d_{12}=2.32$ Å and the dashed line corresponds to $d_{12}=2.42$ Å. Clearly, the DOS of the middle layer of the slab is quite bulk like, and the shift with d_{12} is very small, while the surface-layer DOS is significantly different from that of the middle layer and is very sensitive to d_{12}. By increasing d_{12}, the vibrational frequencies of the first layer ''shift'' downward, which results in a decrease of the vibrational free energy as shown in Fig. 2. The vibrations of atoms in the second layer also ''soften'' by increasing d_{12} and contribute to the decrease of the vibrational free energy. Figure 5 shows the ''shift'' of the phonon DOS in the top layer with d_{12} for different vibrational modes. It can be seen that as d_{12} increases from 2.32 Å to 2.42 Å, not only the vibrational modes that are perpendicular to surface, but also those parallel to surface, shift downward. The shift of the perpendicular modes reflects the anharmonicity of the interlayer potential E normal to the surface, while the shift of the parallel modes is due to the flattening of the corrugation of the potential parallel to the surface. The latter effect implies that

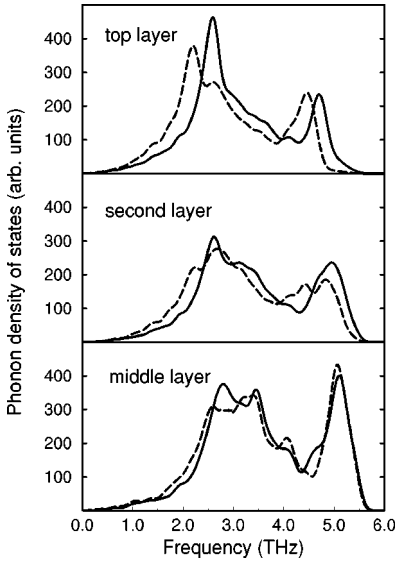

FIG. 4. The phonon density of states (DOS) of different atomic layers. Solid lines are for $d_{12}=2.32$ Å; dashed lines are for $d_{12}=2.42$ Å.

anharmonicity of the interatomic potential at a surface is a somewhat complicated effect where the x, y, and z degrees of freedom are not independent. The modes perpendicular to the surface (corresponding to the Rayleigh wave) are mainly located in the low frequency range and provide a smaller contribution to the DOS. The parallel modes have relatively higher frequencies and occupy a larger portion of the total DOS.

As discussed above in Fig. 2, the increase of $-\partial F_{\mathrm{vib}}/\partial d_{12}$ with temperature determines the expansion of d_{12}. In Fig. 6 the different contributions to $-\partial F_{\mathrm{vib}}/\partial d_{12}$ coming from perpendicular and parallel modes are analyzed. It can be seen that the contribution of the parallel modes to $-\partial F_{\mathrm{vib}}/\partial d_{12}$ is larger than the one of perpendicular modes and that the difference between the contributions from parallel and perpendicular modes increases with temperature. This is in agreement with previous findings.[9,13] Note, however, that this effect is not general and in other systems, as for instance the Be(0001) surface,[19] the ''softening'' of parallel modes plays

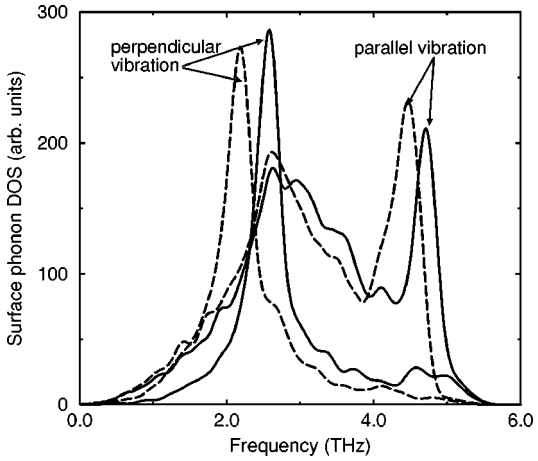

FIG. 5. The shift of phonon DOS at surface from different vibrational modes with different d_{12}. The solid lines are for $d_{12}=2.32$ Å and dashed lines are for $d_{12}=2.42$ Å.

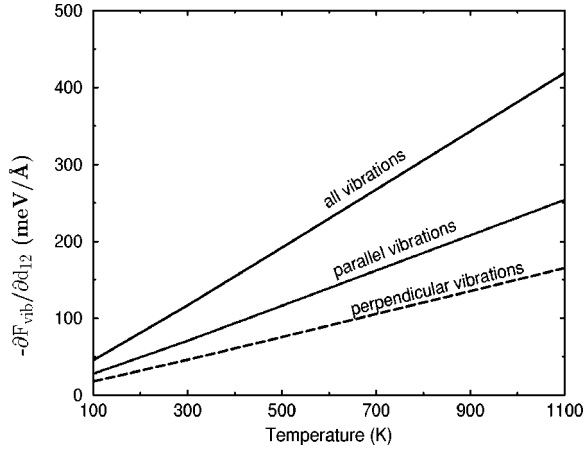

FIG. 6. Contributions to the vibrational free energy from different vibrational modes.

a minor role. Altogether, the enhanced thermal expansion of d_{12} at Ag(111) surface is governed by the anharmonicity of the interlayer potential normal to the surface as well as the ''softening'' of the parallel modes with the increase of d_{12}.

Finally we show in Fig. 7 the surface phonon band structure corresponding to the geometry obtained for $T=300$ K. The thickness of the slab has been extended to 30 atomic layers in order to decouple the surface vibrations that penetrate deeply in the bulk, by inserting in the middle of our slab a number of layers with bulk-like force constants. The lowest surface-mode branch S_1 which lies below the bulk bands is the Rayleigh wave. It is primarily associated with vibrations normal to the surface [shear-vertical (SV) mode, compare also Fig. 5]. The gap mode S_3 is primarily a ''shear-horizontal'' (SH) mode which is associated with vibrations in the direction transverse to $\mathbf{q}_{\|}$ and parallel to the surface. The surface modes S_2 and S_4 are primarily longitudinal modes which are associated with vibrations along the direction parallel to $\mathbf{q}_{\|}$. The calculated frequencies of the Rayleigh mode S_1 are in good agreement with experimental data from helium scattering.[20]

IV. CONCLUSION

Our calculation of the thermal properties of Ag(111) surface are in quantitative agreement with the enhanced thermal expansion found in the experiments. This behavior is found to be determined by two effects: (i) the anharmonicity of the

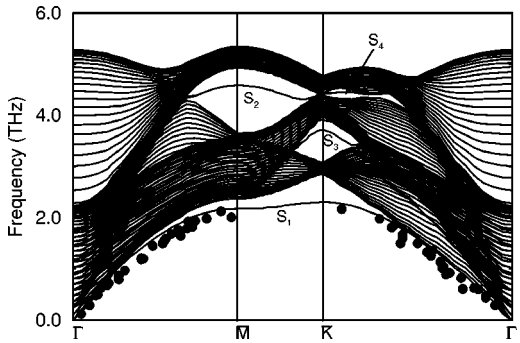

FIG. 7. Calculated phonon dispersion of a 30-layer slab modeling an Ag (111) surface.

interlayer potential normal to the surface and (ii) the decrease of the vibrational free energy with increasing d_{12}. The latter effect reflects not only the anharmonicity of the interlayer potential normal to the surface, but also the flattening of the corrugation of the interlayer potential parallel to the surface with the increase of d_{12}. A recent calculation using the EAM (Ref. 10) shows that the interlayer spacing d_{12} increases very weakly between $T=0$ K and 1100 K. This significant difference to our *ab initio* result is due to two reasons: (i) The **k**-summation in Ref. 10 was done incorrectly; and (ii) the EAM lacks some important aspects of the quantum mechanical nature of electrons.[21] With respect to (i) we note that the surface Brillouin zone has 6 K points (the corners) and 6 M points (the midpoints of the edge lines). However, each corner point belongs to three zones, and each M point belongs to two zones. Thus, the contributions from Γ, K, and M should be added with the weighting factors: 1 (for Γ), 2 (for K), and 3 (for M). In Ref. 10 the following weights had been used: 1 (for Γ), 6 (for K), and 6 (for M). This gives a clearly incorrect description of the **k**-summation.

Note added. In a recent publication[19] it was argued that the validity of the approach of Narasimhan and Scheffler[9] and Cho and Scheffler[22] was unclear. In the present paper we have shown that their ''three-mode-approximation'' overestimates the size of the effect but gives a correct account of the physics.

ACKNOWLEDGMENTS

One of the authors (J.J.X.) would like to acknowledge the financial support from Alexander von Humboldt foundation in Germany. Two of us (S.B. and S.dG.) have done this work in part within the *Iniziativa Trasversale Calcolo Parallelo* of INFM. We thank P. Ruggerone for helpful discussions.

*Present address: T-11, MS-B262, Theoretical Division, Los Alamos National Laboratory, Los Alamos, NM 87545. Electronic address: xie@viking.lanl.gov

[1] R. E. Allen and F. W. de Wette, Phys. Rev. **179**, 873 (1969).
[2] Y. Cao and E. Conrad, Phys. Rev. Lett. **65**, 2808 (1990).
[3] J. W. M. Frenken, F. Huusen, and J. F. van der Veen, Phys. Rev. Lett. **58**, 401 (1987).
[4] G. Helgesen, D. Gibbs, A. P. Baddorf, D. M. Zehner, and S. G. J. Mochrie, Phys. Rev. B **48**, 15 320 (1993).
[5] P. Statiris, H. C. Lu, and T. Gustafsson, Phys. Rev. Lett. **72**, 3574 (1994).
[6] K. H. Chae, H. C. Lu, and T. Gustafsson, Phys. Rev. B **54**, 14 082 (1996).
[7] K. Pohl, J.-H. Cho, K. Terakura, M. Scheffler, and E. W. Plummer, Phys. Rev. Lett. **80**, 2853 (1998).
[8] L. J. Lewis, Phys. Rev. B **50**, 17 693 (1994).
[9] S. Narasimhan and M. Scheffler, Z. Phys. Chem. (Munich) **202**, 253 (1997).
[10] A. Kara, P. Staikov, A. N. Al-Rawi, and T. S. Rahman, Phys. Rev. B **55**, R13 440 (1997).
[11] J. Xie, S. de Gironcoli, S. Baroni, and M. Scheffler, preceding paper, Phys. Rev. B **59**, 965 (1999).
[12] S. Baroni, P. Giannozzi, and A. Testa, Phys. Rev. Lett. **58**, 1861 (1987); P. Giannozzi, S. de Gironcoli, P. Pavone, and S. Baroni, Phys. Rev. B **48**, 3156 (1993).
[13] J. Xie and M. Scheffler, Phys. Rev. B **57**, 4768 (1998).
[14] D. M. Ceperley and B. J. Alder, Phys. Rev. Lett. **45**, 566 (1980) as parametrized by J. P. Perdew and A. Zunger, Phys. Rev. B **23**, 5048 (1981).
[15] X. Gonze, R. Stampf, and M. Scheffler, Phys. Rev. B **44**, 8503 (1991).
[16] M. Methfessel and A. T. Paxton, Phys. Rev. B **40**, 3616 (1989).
[17] C. Kittel, *Introduction to Solid State Physics*, 6th ed. (Wiley, New York, 1986).
[18] S. Biernacki and M. Scheffler, Phys. Rev. Lett. **63**, 290 (1989).
[19] M. Lazzeri and S. de Gironcoli, Phys. Rev. Lett. **81**, 2096 (1998).
[20] R. B. Doak, U. Harten, and J. P. Toennies, Phys. Rev. Lett. **51**, 578 (1983).
[21] ''Embedded atom method'' is one name out of several names for essentially the same approach. Others are, e.g., bond cutting model, effective medium theory, and glue model. All these ''bond cutting models'' neglect in their standard applications the shell structure of atoms ($s,p,d,\ldots$ electrons) and describe the interaction between atoms by a sum of pair potential and effective atomic-many-body contributions. Thus, when the kinetic energy of electrons and/or a hybridization of $s,p,d,\ldots$ orbitals is changing, ''bond cutting models'' are likely to fail.
[22] J. H. Cho and M. Scheffler, Phys. Rev. Lett. **78**, 1299 (1997).